https://doi.org/10.56801/MME1068

Effect of SiC Particles on Mechanical Properties of Stir-Friction Welded Al/SiC Composites Fabricated by Lost Foam Casting

Moe Rabea[1], Mushtaq Albdiry[2]

[1]*Department of Industrial and Manufacturing Engineering, College of Engineering, California State Polytechnic University, United States, Email: malrabea@cpp.edu*
[2]*Department of Materials Engineering, College of Engineering, University of Al-Qadisiyah, Iraq, Email: mushtaq.taleb@qu.edu.iq*

Received: 21-01-2024; Revised: 03-02-2024
Accepted: 22-02-2024; Published: 07-03-2024

Abstract: This study investigates the effects of inserting sub-micron hard silicon carbide (SiC) particles in a welded zone of aluminum (Al)/SiC metal matrix composite. Two parts of Al/35 wt. % SiC composites fabricated by lost foam casting (LFC) were welded together using friction stir welding (FSW) process. As reinforcement, 5 wt. % of SiC particles were inserted in the welding zone of the composites to enhance their microhardness and tensile strength as well as alleviate their thermal shock and weight loss/abrasion resistance. The optical images showed a good dispersion of SiC particles in the welded zone that resulted in a higher microhardness and tensile strength. The presence of well-dispersed SiC particles exhibited a good shock resistance of the composite even at higher temperatures, and lower weight loss (better corrosion performance) under salt spray test and a harsh 5% w/v NaCl solution for the presence of a hard equilibrium SiC and Al_4C_3 phases with further addition of SiC particles.

Keywords: FSW; lost foam casting; SiC; mechanical properties; metal matrix composite.

1. Introduction

Aluminum alloys consider one of the most applicable engineering materials/alloys widely used in construction, automobile, marine and aerospace as well as mineral processing industries for their light weight, good thermal conductivity and moderate mechanical properties [1]. Among these alloys are heat treatable and corrosion resistant alloys-based SiC metal matrix composites (MMCs) which generally used in X-37B and X-38 aircrafts parts like nose cone, leading edge wing and engine components [2, 3]. However, such complex shapes are difficult to be fabricated by traditional casting processes and hence some of their parts are required to be joined together by appropriate joining method [4]. Friction stir welding (FSW) is one of a solid-state welding method mostly used to weld aluminum and titanium alloys. In the FSW process, the welding is completed via a FSW tool that generates heat due the friction between its pin and the workpieces resulted in softening the material around the pin [5]. The strength of the metallic lap joints welded by FSW is dependent on the microstructural changes in and around weld zone in addition to the size/distribution of the inserted reinforced materials, properties of the weldment, and welding parameters including tool dimensions, structure of the workpiece and temperature distribution [6, 7]. Different microstructures having various

morphologies and hence various mechanical properties can be noticed in the friction stir welding zone of aluminum alloy. These changes in morphologies resulted from the generation of hard intermetallic compounds in the interfacial region [8]. Compared to the base aluminum alloy, it was found that the tensile strength, elongation and Vickers micro-hardness of the stir welded alloy increased by 92%, 54%, and 75% respectively for the formation of a very fine grain size at the nugget zone and the uniform dispersion of reinforcement particles [9]. Interestingly, inserting ceramic powder in the welding joint of aluminum alloys also resulted in higher micro-hardness and strength owing to the uniform distribution of strengthening precipitates in the zone [10]. Effects of hardening parameters on tensile and impact strengths of Al 2024 alloy welded by friction stir process were conducted [11].

The incorporation of hard micro-size particles in the welding zone of AA2024 alloy along with optimizing FSW parameters (heat input and tool speed) exhibited dramatic recrystallization of the nugget zone led to the formation of equiaxed grains and thereby higher mechanical properties [12].

In particular, Liu et al. [13] conducted that inserting 8% SiC particles in the welding zone of Al-Mg/SiC MMCs led to refine their grains nucleation and enhanced tensile and micro-hardness strengths. Similarly, considerable improvements in hardness and mechanical properties were confirmed in [14], and attributed for the role of SiC reinforcement in Al MMCs in lowering grain boundary fractions and misorientation i.e., rearrangement of dislocation substructures. Nonetheless, there is no study conducted on the role of inserting SiC particles in the welding zone of similar Al/SiC MMCs during the FSW process. Therefore, this study comprehensively conducts the role of inserting SiC microparticles in the weld interface of Al/SiC MMCs welded by FSW process. The microstructural characteristics, tensile strength and Vickers micro-hardness of Al alloy, and base Al/SiC MMCs (Al/SiC_b) fabricated by lost foam casting were determined and compared to the welded Al/SiC MMCs joints having 5 wt. % SiC particles inserted in the welding zone (Al/SiC_S). The effects of SiC particles on the abrasion resistance (weight loss) of the welded MMCs subjected to spray 5 % w/v NaCl salt solution as well as their thermal shock behavior at different temperatures were also conducted.

2. Materials and Method

2.1 Materials Used

In this study, aluminum (Al) alloy having an average particle size of 50 μm and a chemical composition shown in Table 1 was used as a base alloy. Silicon carbide (SiC) particles having an average particle size of 20 μm were employed as reinforcement.

Table 1. *The chemical composition (wt. %) of aluminum alloy used in the study.*

Si	Fe	Cu	Mn	Mg	Cr	Zn	Ti	Sn	Pb	Ni	Al
0.067	0.085	0.014	0.12	0.75	0.0001	0.015	0.2	0.001	0.001	0.008	Rem.

2.2 Fabrication of Al/SiC composite

To fabricate Al/SiC metal matrix composite, Al alloy was melted in an induction furnace using ceramic crucible at 780°C with a total size of the prepared batch is 750 cm^3. The SiC particles were added by 35 wt. % to the patch, well stir-mixed and poured in a small mold having a Styrofoam pattern according to lost foam casting. Upon cooling, squared plates of 150 mm ×150 mm dimensions and thickness of 5 mm were prepared for the following welding process.

2.3 Friction stir welding of Al/SiC composite

Friction stir welding (FSW) as illustrated in Figure 1 was applied to join two similar Al/SiC MMCs workpieces (butt joints) at a rotation speed of 900 rpm. To investigate the effects of SiC particles on the materials properties of the welded joints, a 5 wt. % SiC particles were inserted in the middle butting welding zone during the friction stirring process. Thereafter, a post-welding heat treatment was performed at 200ºC for all welded joints to relief any residual stresses and recrystallization.

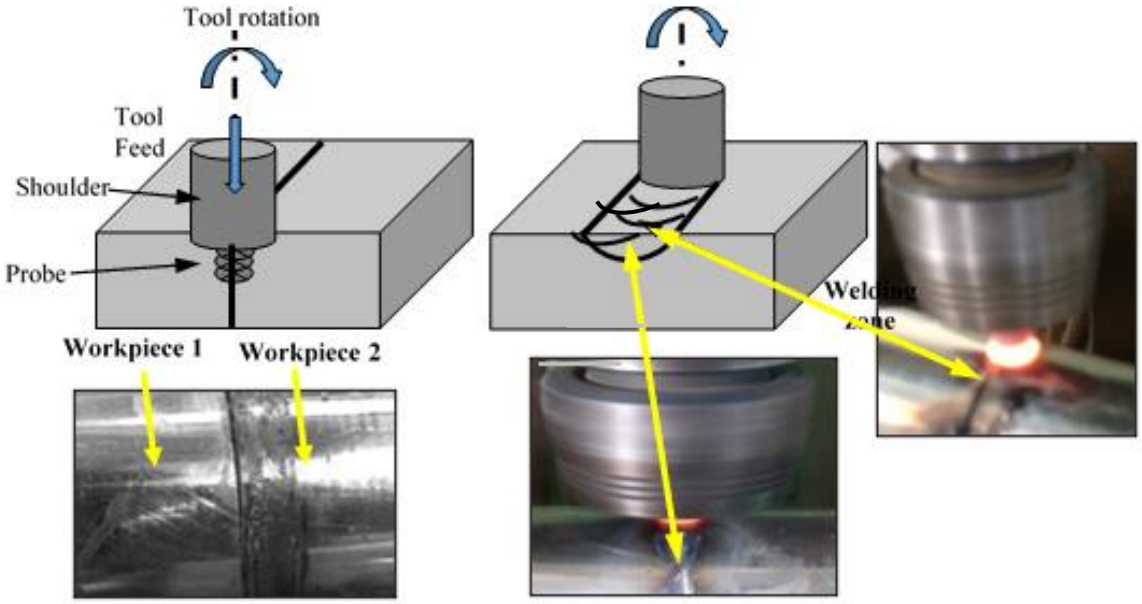

Figure 1. *Friction stir welding process of two Al/SiC composite workpieces.*

2.4 Materials characterizations

To prepare testing samples, various specimens at different dimensions were sectioned from the welding zone of the Al/SiC MMCs using CNC milling machine for the microscopic examination, micro-hardness, and tensile strength. The optical microscopic samples for Al/SiC_b MMCs and Al/SiC_S MMCs as shown in Figure 2a & 2b, respectively, were polished on sand papers of various grades and then cloth polished with fine alumina powder on a revolving wheel. Tensile test for the butt welded joints of the MMCs as shown in Figure 2c, was preformed using universal computerized testing machine at room temperature and a strain rate of 2 mm/min. Vickers micro-hardness tester type HM-200 was used to measure the micro-hardness of the prepared samples (Figure 2d) applying a load of 500 g for at least five testing measured at different points of each sample. The thermal shock test indicated by the weight loss measurement of the welded composites joints was carried out at different temperatures of 200°C, 250°C, 300°C, 350°C, 400°C, 450°C and 500°C. in these temperatures, all samples are lasted for 15 min and then water quenched. The abrasion resistance as indicated by the weight loss for aluminum alloy and its welded MMCs was characterized using a 450 L salt spray chamber having a 0.4 L/h.m^3 flow capacity. All samples were being in direct exposure by concentrated 5% w/v NaCl salt at 50°C, 15° angle, and 1 bar pressure by a nozzle in the chamber to accelerate the abrasion and weight losing of the prepared samples. The weight loss of the welded composites was determined after an exposure time of 50 hr. at a humidity set at 50%.

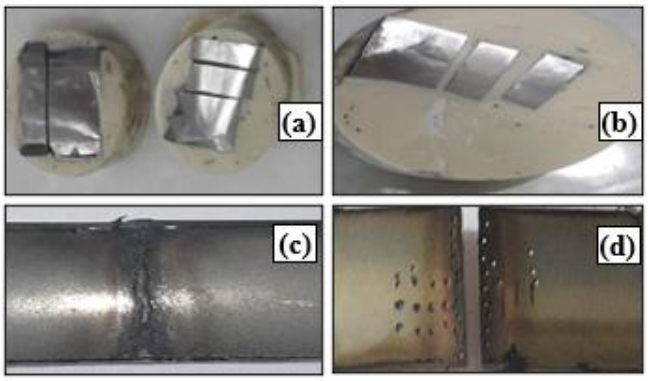

Figure 2. *The microscopic specimens for Al/SiC$_b$ MMCs (a) Al/SiC$_S$ (b); and tensile testing (c) and micro-hardness specimens after testing (d).*

3. Results and Discussion

3.1 Microstructural characteristics

Figure 3 illustrates the optical microscopic (OM) images for Al alloy and the cross-sectional Al/SiC MMCs welded by the FSW process before and after inserting further 5 wt. % SiC particles. It is clearly shown that the microstructure of the base Al alloy (Figure 3a) fabricated by a lost foam casting, had a homogeneous fine-grained structure of α-Al solid solution and precipitates of intermetallic phases which is in conformance with [15]. The microstructure of the welded Al/SiC composites (Figure 3b) shows some clusters of SiC particles for the less degree of bonding between the SiC and Al matrix, resulting in the generation of micro-porosities. Additionally, the microstructure also indicates the formation of intermetallic Al_4C_3 compounds on the boundary layers with the appurtenance of various welding defects such as voids, hook, and groove. However, with the further addition of SiC in the welding zone of Al/SiC$_S$ MMCs, its microstructure (Figure 3c) indicates a good bonding between SiC particles and the molten matrix. This was attributed to the further addition of carbides led to interact with the high content of Mg content in the base Al alloy, and consequently led to enhance the distribution of precipitants in the structure of the welded Al/SiC$_S$ composites [16]. Furthermore, Figure 3d clearly shows the uniform structure of the intermetallic compounds and well-distributed SiC particles in the single-pass FSW welded zone of Al/SiC$_S$ MMCs.

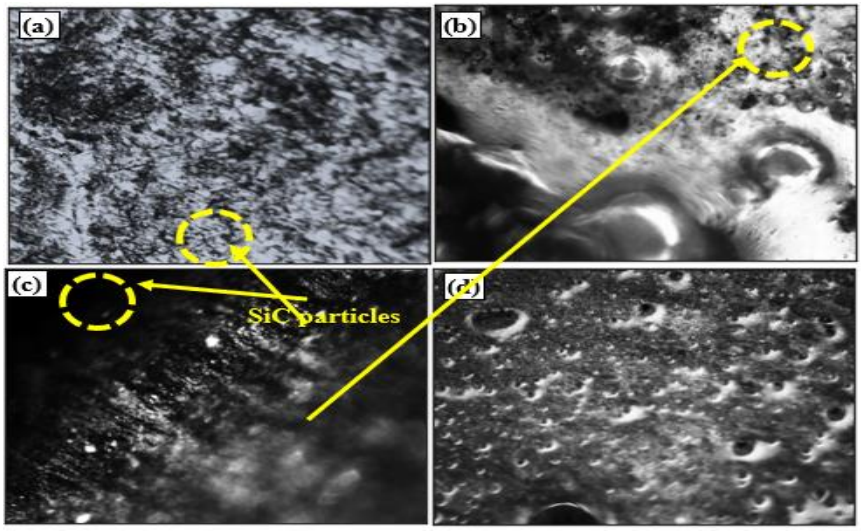

Figure 3. *The optical microscopic images for Al alloy (a), the welded interface of Al/SiC$_b$ MMCs (b) the welded interface of Al/SiC$_S$ (c and d).*

3.2 Microhardness and Tensile Properties

The Vickers microhardness (HV) values of Al alloy, the FSW welded Al/SiC_b and the FSW welded Al/SiC_S MMCs are given in Figure 4. The microhardness of Al alloy was 67 HV, has almost doubled to 112 HV with the reinforcement of 35 wt. % SiC particles in Al/SiC_b MMCs for the presence of hard SiC particles. The micro HV value has reached 121 HV for the FSW welded Al/SiC_S due to the homogeneous SiC particle distribution that generated dislocation pinning and thereby a refined grain microstructure.

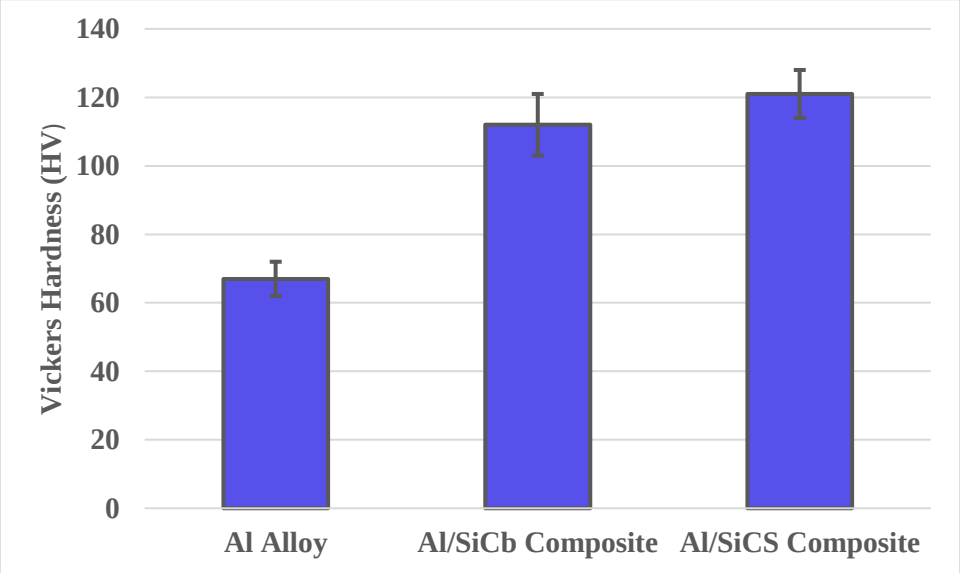

Figure 4. *Micro-hardness of Al alloys and its FSW welded Al/SiC_b and Al/SiC_S composites*

Results of the ultimate tensile strength (UTS) of Al alloy and the FSW welded Al/SiC_b and Al/SiC_S composites are shown in Figure 5. From the Figure, the tensile strength of Al alloy was measured at least five measurements and its average value is 208±12 MPa. This tensile strength of SiC-reinforced Al alloy (Al/SiC_b) has significantly increased to reach 266±18 MPa by 28 % enhancement for the role of hard SiC particles and presence of different intermetallic carbides phases along with the refined-grain size structure. The tensile strength of Al/SiC_S MMCs that had additional 5 wt. % SiC in the welding zone, has further increased to 272±20 MPa due to the increased SiC content that contributed to create more dislocations (or dislocation movement) that gather in their crack/micro-crack path. This results in an increase plastic deformation that acts to carry further loads before fracture [17-19]. Similar values of the increased tensile strengths were found for Al alloy after the incorporation of SiC in aluminum MMCs fabricated by spark plasma sintering [20, 21], and were attributed for the re-precipitation and the good interfacial bonding between Al (matrix) and SiC particles (reinforcement) throughout the aluminum matrix that caused perfect strengthening mechanism due to the increased dislocation densities and efficient load transferring from the Al matrix to the Al/SiC interface and then to the intermetallic and SiC phases. However, further increase of SiC content tends to increase SiC precipitants on the boundary layers (or the interface) and hence reducing bonding strength. Therefore, this study was only committed to determine the role of 5 wt. % SiC on the microstructure, mechanical characteristics and thermal shock and weight loss of Al/SiC MMCs.

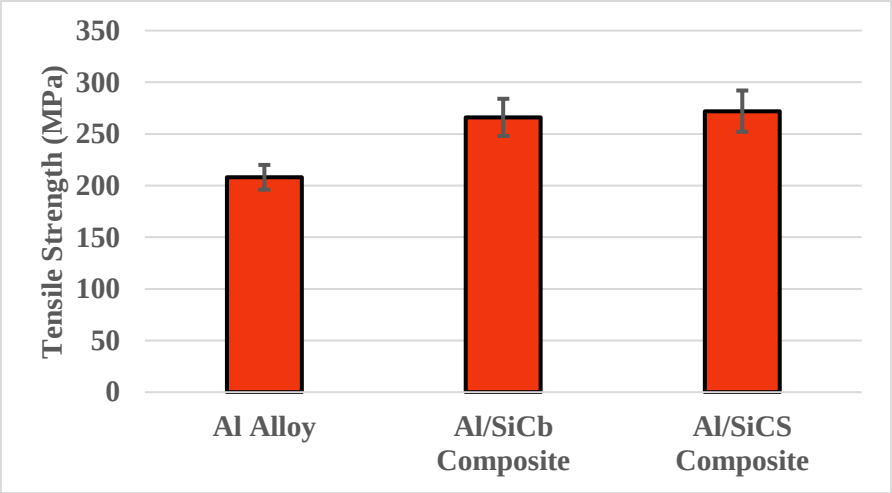

Figure 5. *Tensile strengths of Al alloys and its FSW welded Al/SiC$_b$ and Al/SiC$_S$ composites*

3.3 Thermal Shock and Spray Chamber

The thermal shock behavior indicated by the weight loss (or abrasion resistance) of Al alloy and its FSW welded Al/SiC$_b$ and Al/SiC$_S$ composites joints in relation to different temperatures (200°C, 250°C, 300°C, 350°C, 400°C, 450°C and 500°C) is shown in Figure 6. From the Figure, it is clearly observed that all materials suffered from an increase weight loss with increasing temperature regardless which one has behaved the best. The weight loss of aluminum alloy was the highest while the welded zones of Al alloy reinforced by 35 % SiC (Al/SiC$_b$) composites had lower weighting loss for their higher hardness and strength due the presence of hard SiC particles and the generated intermetallic phases thereof. Inserting of 5 wt. % SiC in the welding zone in Al/SiC$_S$ resulted in better thermal shock behavior and their weighting loss was the lowest. This is attributed again for the better microhardness, uniform dispersion of SiC particles in the welding zone and the presence of hard SiC phase. It was similarly reported that inserting graphene particles in Al/SiC composites demonstrated higher tensile/hardness properties and corrosion/abrasion resistance for the prefect interface cohesion by lowering defective interface between Al matrix and graphene/SiC reinforcement and presence of homogenous hard fine-grained structure [22].

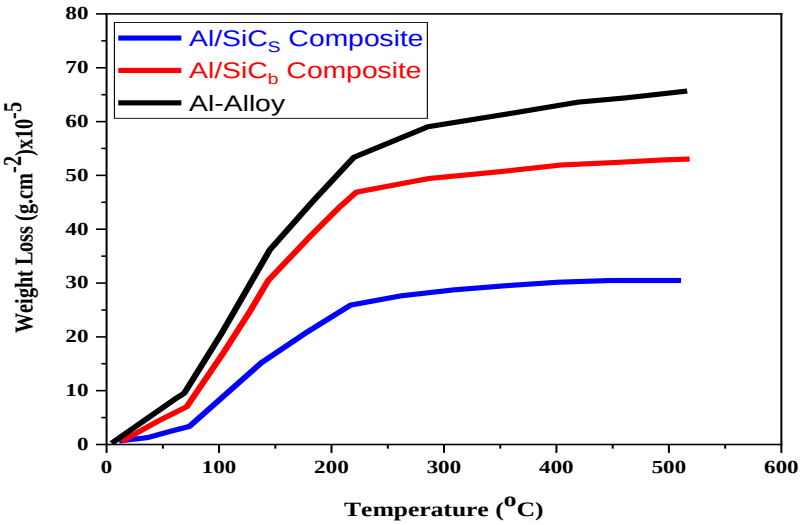

Figure 6. *The weight loss measurements of Al alloys and its FSW welded Al/SiC$_b$ and Al/SiC$_S$ composites due to the thermal shock of heating at different temperatures and water quenching.*

Furthermore, measurements of the weight lost for all composites sprayed by concentrated 5 % w/v NaCl salt solution at 50°C for 50 hr and 1 bar pressure are illustrated in Figure 7. It is clearly noticed that aluminum alloy has suffered from a higher range of weighting lost after the exposure to a direct spray salt solution compared to its FSW welded SiC MMCs. The role of hard SiC particles in reinforcing Al alloy was obvious where both the welded Al/SiC_b and Al/SiC_S relatively exhibited a very lower weight loss indicating a higher corrosion/abrasion resistance at high corroded 5 % NaCl solution. In numbers, the weight loss of Al alloy was found to be $105\pm7\times10^{-5}$ g/cm^{-2} has dropped to only $39\pm5\times10^{-5}$ g/cm^{-2} for the FSW welded Al/SiC_b and further reduction to $13\pm3\times10^{-5}$ g/cm^{-2} for the FSW welded Al/SiC_S metal matrix composites having additional 5 wt. % SiC particles. This significant weight loss of Al alloys was possibly ascribed to the generation of micro-pores/holes and consequently micro-cracks in these alloys due to insufficient melting parameters of the used lost foam casting [23-25]. On the other hand, the significant reduction in the weight loss and hence better corrosion/abrasion resistance of the welded butt Al/SiC composite joints in front of the direct sprayed 5 % NaCl salt solution is returned again for the good interfacial cohesion between the aluminum matrix and SiC reinforcement as well as the hard well-dispersed SiC particles near the surface and presence of uniform intermetallic (bonding) phases [26]. Interestingly. It was proved that fabricating Al/SiC MMCs using multi-pass FSW resulted in strain-free fine grains, well-dispersed and totally fragmenting of SiC in Al alloy structure which in turn caused a higher tensile and Vickers's microhardness and better corrosion resistance [27].

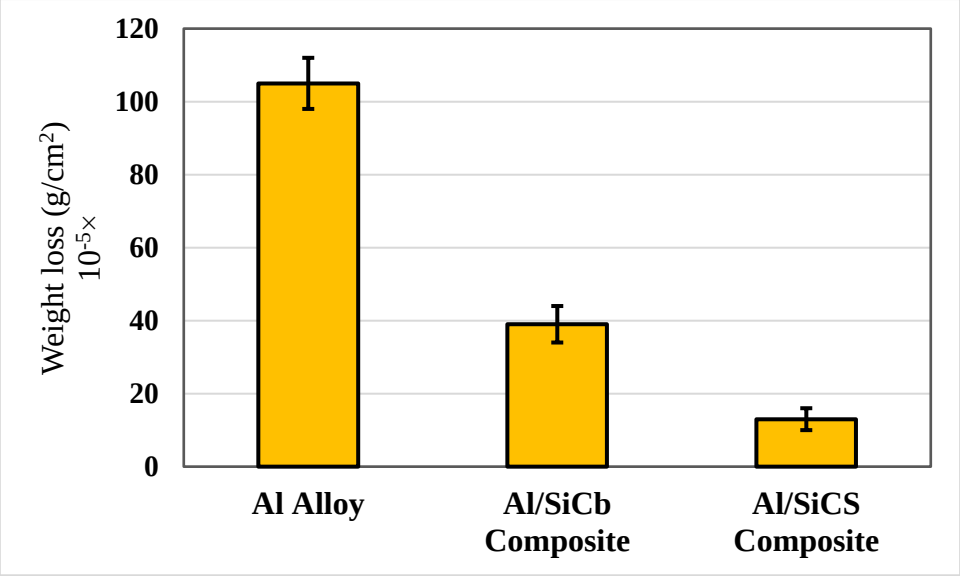

Figure 7. *The weight loss measurements of Al alloys and its FSW welded Al/SiC_b and Al/SiC_S composites after the direct salt spray by 5 % w/v NaCl solution.*

4. Conclusions

This study conducts the fabrication of Al alloy-reinforced by 35 % SiC metal matrix composite (MMCs) by the lost foam casting (LFC), and also investigates the role of inserting 5 % SiC particles in the welded zone of the welded FSW Al/SiC MMCs. The results revealed that the successful fabrication of Al/SiC MMCs by LFC with a homogeneous fined-grain structure. inserting of SiC particles in the welding interface zone exhibited a considerable increase in the Vickers microhardness and tensile strength of the reinforced Al/SiC MMCs which was ascribed for the presence of hard uniformly dispersed SiC and intermetallic phases in the aluminum matrix as well as the FSW led to refine the grain particles of the pre-casted composites. This enhancement in mechanical properties also caused in a better

corrosion/abrasion resistance and higher thermal shock resistance of the Al/SiCS compared to the aluminum alloy. Upon the results obtained in this study, it is well recommended to utilize different type of hard reinforcements to be inserted in the welding zone of welded FSW MMCs in to be inserted in the welding zone of welded FSW MMCs in order to enhance their density, microhardness and tensile strength as well as enhance the thermal shock behavior and weight loss due to corrosion/abrasion test.

References

1. Khalid, M.Y., R. Umer, and K.A. Khan, *Review of recent trends and developments in aluminium 7075 alloy and its metal matrix composites (MMCs) for aircraft applications.* Results in Engineering, 2023. **20**: p. 101372.
2. Zhang, K., et al., *Joining of C_f/SiC Ceramic Matrix Composites: A Review.* Advances in Materials Science and Engineering, 2018. **2018**: p. 6176054.
3. Albdiry, M. and H. Alethari, *Effect of alumina inclusions on microstructure and mechanical properties of 62 WC, 32 (Ti-W) C and 6 Co compacts.* International Journal of Microstructure and Materials Properties, 2012. **7**(4): p. 329-340.
4. Çam, G. and G. İpekoğlu, *Recent developments in joining of aluminum alloys.* The International Journal of Advanced Manufacturing Technology, 2017. **91**(5): p. 1851-1866.
5. Çam, G., *Friction stir welded structural materials: beyond Al-alloys.* International Materials Reviews, 2011. **56**(1): p. 1-48.
6. Wang, X., et al., *Effect of welding parameters on the microstructure and mechanical properties of linear friction welded Ti-6.5Al-3.5Mo-1.5Zr-0.3Si joints.* Journal of Manufacturing Processes, 2019. **46**: p. 100-108.
7. Albdiry, M.T. and A.I. Almosawi, *Effect of compacting pressure on microstructure and mechanical properties of carbide cutting tools.* Powder Metallurgy, 2011. **54**(5): p. 585-591.
8. Abdollah-Zadeh, A., T. Saeid, and B. Sazgari, *Microstructural and mechanical properties of friction stir welded aluminum/copper lap joints.* Journal of Alloys and Compounds, 2008. **460**(1): p. 535-538.
9. Salih, O.S., et al., *Microstructure and mechanical properties of friction stir welded AA6092/SiC metal matrix composite.* Materials Science and Engineering: A, 2019. **742**: p. 78-88.
10. Albdiry, M.T., H. Ku, and B.F. Yousif, *Impact fracture behaviour of silane-treated halloysite nanotubes-reinforced unsaturated polyester.* Engineering Failure Analysis, 2013. **35**: p. 718-725.
11. Karthikeyan, P., D. Thiagarajan, and K. Mahadevan, *Study of Relation between Welding and Hardening Parameters of Friction Stir Welded Aluminium 2024 Alloy.* Procedia Engineering, 2014. **97**: p. 505-512.
12. Zhang, C., G. Huang, and Q. Liu, *Quantitative analysis of grain structure and texture evolution of dissimilar AA2024/7075 joints manufactured by friction stir welding.* Materials Today Communications, 2021. **26**: p. 101920.
13. Liu, K., et al., *Effect of SiC addition on microstructure and properties of Al–Mg alloy fabricated by powder and wire cold metal transfer process.* Journal of Materials Research and Technology, 2022. **17**: p. 310-319.
14. Pk, J., et al., *The effect of SiC content in aluminum-based metal matrix composites on the microstructure and mechanical properties of welded joints.* Journal of Materials Research and Technology, 2021. **12**: p. 2325-2339.

15. Thakur, A., et al., *Appearance of reinforcement, interfacial product, heterogeneous nucleant and grain refiner of MgAl2O4 in aluminium metal matrix composites.* Journal of Materials Research and Technology, 2023. **26**: p. 267-302.
16. Kesharwani, R., et al., *Comparison of microstructural, texture and mechanical properties of SiC and Zn particle reinforced FSW 6061-T6 aluminium alloy.* Journal of Materials Research and Technology, 2023. **26**: p. 3301-3321.
17. Du, Y., et al., *Effect of Al content on chemical corrosion resistance of Al/SiC composites.* Ceramics International, 2023. **49**(22, Part B): p. 36928-36934.
18. Al-Adily, K., M. Albdiry, and H. Ammash, *Evaluation of tensile and flexural properties of woven glass fiber/epoxy laminated composites oriented in edgewise and flatwise directions.* Ain Shams Engineering Journal, 2023: p. 102255.
19. Al-Badri, M. and M. Albdiry, *Enhanced electrical properties of ternary CNTs/PANI wrapped by sulfonated graphene nanocomposite for supercapacitor electrodes.* Journal of Materials Science: Materials in Electronics, 2021.
20. Hong, Y., J. Liu, and Y. Wu, *The interface reaction of SiC/Al composites by spark plasma sintering.* Journal of Alloys and Compounds, 2023. **949**: p. 169895.
21. Al-badri, M. and M. Albdiry, *Electrochemical performance of ternary s-GN/PANI/CNTs nanocomposite as supercapacitor power electrodes.* Periodicals of Engineering and Natural Sciences, 2020. **8**(4): p. 2484-2489.
22. Zeng, M., et al., *Effects of 3D graphene networks on the microstructure and physical properties of SiC/Al composites.* Ceramics International, 2023. **49**(5): p. 8140-8147.
23. Albdiry, M. and F. Mahdi, *Bimetallic CoMo and trimetallic CoMoW catalyst supported on γ-Al2O3 for efficient naphtha hydrodesulfurization.* Reaction Kinetics, Mechanisms and Catalysis, 2023. **136**(5): p. 2555-2568.
24. Albdiry, M.T. and B.F. Yousif, *Morphological structures and tribological performance of unsaturated polyester based untreated/silane-treated halloysite nanotubes.* Materials & Design, 2013. **48**: p. 68-76.
25. Albdiry, M.T. and M.F. Almensory, *Failure analysis of drillstring in petroleum industry: A review.* Engineering Failure Analysis, 2016. **65**: p. 74-85.
26. Karthikraja, M., et al., *Corrosion behaviour of SiC and Al2O3 reinforced Al 7075 hybrid aluminium matrix composites by weight loss and electrochemical methods.* Journal of the Indian Chemical Society, 2023. **100**(5): p. 101002.
27. Mehdi, H. and R.S. Mishra, *Effect of multi-pass friction stir processing and SiC nanoparticles on microstructure and mechanical properties of AA6082-T6.* Advances in Industrial and Manufacturing Engineering, 2021. **3**: p. 100062.